EXOSC10 mediated RNA degradation sculpts the transcriptome during oocyte growth-to-maturation transition

SUPPLEMANTERY FIGURES AND TABLES

Figure S1. Characterization of *Exosc10* oocyte-conditional knockout mice. (**A**) Schematic of the strategy to generate *Exosc10* knockout allele using CRISPR/Cas9 in which two gRNAs were used to delete exons 4-10. (**B**) Schematic of mRNAs generated from the floxed and cKO alleles. In the latter, exons 4-10 are absent, and an early termination occurs in exon 11. (**C**) Number of pups with indicated genotypes. No *Exosc10* homozygous null pups survived to term. (**D**) qRT-PCR of *Exosc10* in single oocytes obtained from controls and cKO females. Two primer pairs were used (see **B)**. Primer pair 1, shown here, detects the region deleted after loxP recombination; primer pair 2 detects region shared by the mRNAs transcribed from the *Exosc10* floxed and cKO allele. (**E**) Representative ovaries (12 w/o) dissected from control and cKO mice. (**F**) Ovary/body weight ratio of control and cKO females (12 w/o). Numbers of ovaries indicated below each group. (**G**) Histology of periodic acid-Schiff stained ovaries in **E**. (**H**) Quantification of fully-grown oocytes in single (2 μm) sections from **G**. Number of ovaries indicated below each group. (**I**) Diameter of control and cKO oocytes. The horizontal lines represent the median and quartiles. (**J**) *Ex vivo* maturation of control and cKO GV oocytes through meiosis (MI, MII). Number of oocytes indicated below each group. (**K**) Number of ovulated eggs collected from control and cKO female oviducts after hormonal stimulation with eCG and hCG. Number of females indicated below each group. (**L**) Immunostaining of microtubule-organizing center (MTOC) proteins pericentrin (PCNT) and γ-tubulin, indicated by arrowheads. (**M**) Confocal fluorescence and bright-field images of EXOSC10-mVenus localization during control oocyte maturation and pre-implantation development. (**N**) *Ex vivo* culture of pre-implantation development of the embryos derived from control and cKO female mice. Bright-field images were obtained at E1.5, E2.5 and E3.5. (**O**) Quantification of the embryonic progression at each time point in **N**. In **F**, **H**, **K**, the horizontal lines represent the mean and standard deviation. Scale bars: 1 mm in **E**, **G**; 20 μm in **L**, **M**; 100 μm in **N**. **** P <0.0001, ** P <0.05, two-tailed Student's t-test.

Figure S2. EXOSC10 degrades poly(A) RNA in oocytes. (**A, C, E**) Confocal fluorescence images showing poly(A) RNA FISH, bright-field and DAPI of wildtype oocytes at GV, GV+3hr and MII stages in **A**, of oocytes over expressing *mVenus*, *Exosc10-mVenus or dExosc1-mVenus* cRNA at GV, GV+3hr stages in **C**, and of oocytes derived from controls and cKO females at GV, GV+3hr in **E**. The oocytes at GV+3hr stage were obtained by *ex vivo* culture of GV oocytes in maturation medium for 3 hr. (**B, D, F**). Quantification of overall poly(A) RNA fluorescence of **A**, **C**, **E**, respectively. The horizontal lines represent the mean and standard deviation. In **B**, Nc1, negative control 1, without probe incubation; Nc2, negative control 2, treated by RNase A before probe incubation. Number of oocytes indicated below each group. **** P <0.0001, * P <0.05 in **D** by one-way ANOVA. Scale bars: 20 μm in **A**, **C**, **E**.

Figure S3. Validation of linear amplification of 64 RNA-seq libraries by ERCC RNA spike-in mix. Each scatter plot represents the linear regression of ERCC reads with the original concentration. The red number is the covariant of coefficient and the blue number is the ERCC components (92 in total) detected. Libraries are from GV ctr, control GV oocytes; GV.3_ctr,

control GV oocytes incubated for 3 hr; MII_ctr, control MII oocytes; GV_cKO, cKO GV oocytes; GV.3_cKO, cKO GV oocyte incubated for 3 hr; MII_cKO, cKO MII oocytes.

Figure S4. Over-expression of *Rab5a* and *Rab5c* cRNA failed to phenocopy *Exosc10*^{cKO} oocytes. (**A**) Brightfield images after *ex vivo* culture (0, 3 hr, 20 hr) of wildtype oocytes injected with cRNA of *Rab5a-mVenus*, *Rab5c-mVenus*, *Rab5a-mVenus/Rab5c-mVenus* and *mVenus*. (**B**) Bar grafts of oocyte maturation from GVBD (BD) to MII in **A** in two independent experiments. The total number of oocytes is indicated above each bar graph. (**C-D**) Fluorescent images of oocytes after co-injection of cRNA of *Rab5a-mVenus* and *Rab5c-mVenus* which failed to decrease RAB7. Scale bars: 100 μm in **A**, **C, D**.

Figure S5. Lamin B and lamin A/C pattern in Intact, GVBD (early) and GVBD (late) oocytes. (**A, C**) Representative figures of immunostaining of lamin B and lamin A/C at 0-1 hr, 1-2 hr and 2-3 hr of wildtype GV oocytes during *ex vivo* culture. (**B, D**) Quantification of lamin B and lamin A/C. The horizontal lines represent the median and quartiles.

Figure S6. cAMP level does not increase in *Exosc10*^{cKO} oocytes. (**A**) A bar graph of the mean and standard error of $\log_2$ fold change of *Gpr12* (G protein-coupled receptor 12), *Gpr3* (G protein-coupled receptor 3), *Pde3a* (phosphodiesterase 3A), *Adcy3* (adenylate cyclase 3), *Adcy9* (adenylate cyclase 9) from single oocyte RNA-seq data sets. **** *P* <0.0001, *** *P* <0.001, ** *P* <0.01, * *P* <0.05, n.s. no significance, which are the *P*-adjust values in the DESeq2 analysis. (**B**) Confocal fluorescence images of cAMP in control and Exosc10 cKO GV oocytes. Scale bars: 20 μm.

Table S1. Differential expression analysis of the single oocyte RNA-seq by DESeq2, including GV_cKO vs GV_ctr, GV3h_cKO vs GV3h_ctr, MII_cKO vs MII_ctr, GV3h_ctr vs GV_ctr, MII_ctr vs GV3h_ctr, and cKO_major vs cKO_minor. Each differential analysis result contains the Log_2 fold change, the standard error and the *P*-adjust values of the significantly changed transcripts (*P*-adjust < 0.01).

Figure S1

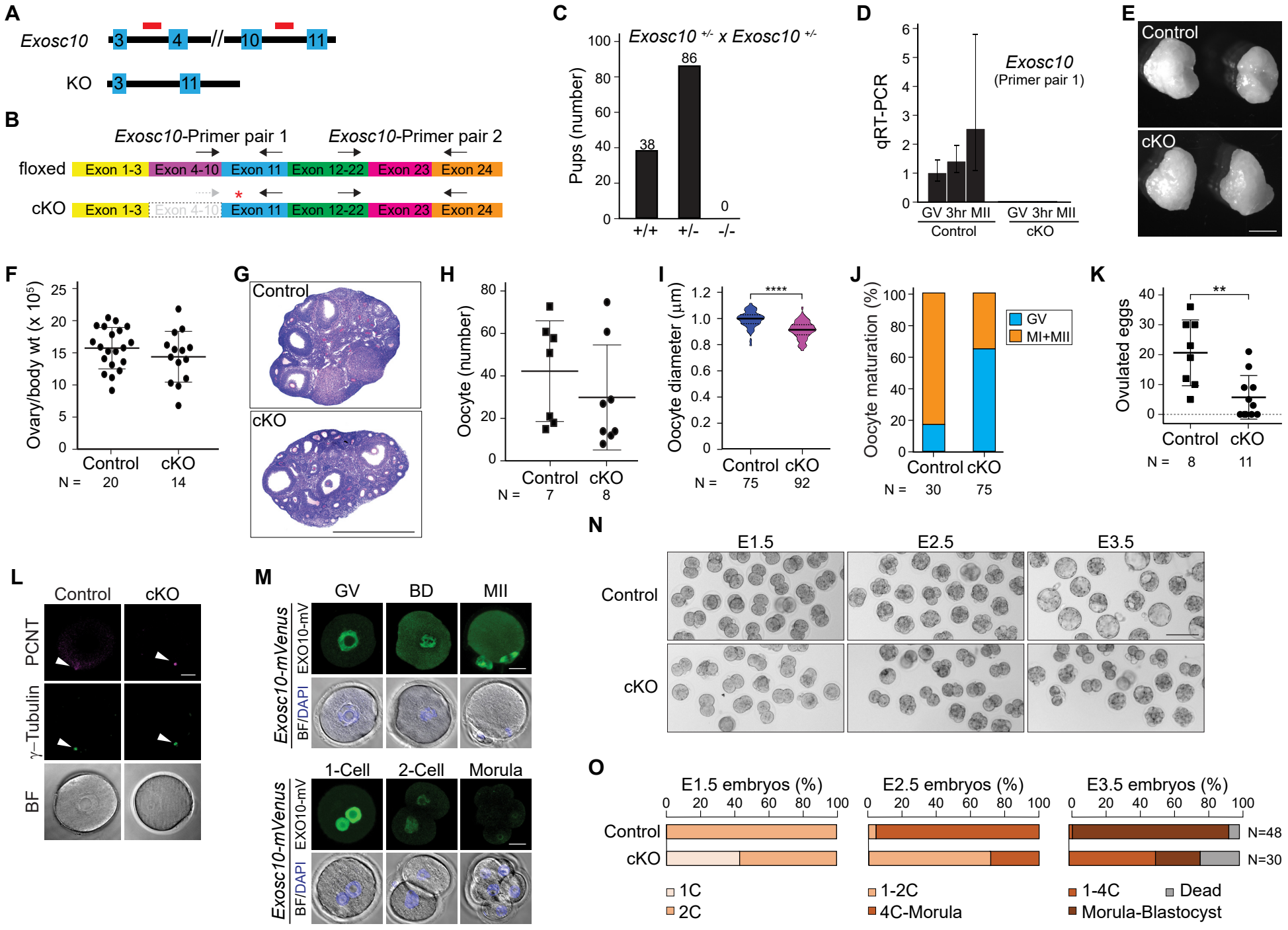
A
Exosc10
3
4
10
11
KO
3
11
B
Exosc10-Primer pair 1
Exosc10-Primer pair 2
floxed
Exon 1-3
Exon 4-10
Exon 11
Exon 12-22
Exon 23
Exon 24
cKO
Exon 1-3
Exon 4-10
Exon 11
Exon 12-22
Exon 23
Exon 24
C
Exosc10 +/- x Exosc10 +/-
Pups (number)
38
86
0
+/+
+/-
-/-
D
qRT-PCR
Exosc10
(Primer pair 1)
GV 3hr MII
Control
GV 3hr MII
cKO
E
Control
cKO
F
Ovary/body wt (x 10^5)
Control
cKO
N = 20 14
G
Control
cKO
H
Oocyte (number)
Control
cKO
N = 7 8
I
Oocyte diameter (µm)
****
Control
cKO
N = 75 92
J
Oocyte maturation (%)
GV
MI+MII
Control
cKO
N = 30 75
K
Ovulated eggs
**
Control
cKO
N = 8 11
L
Control
cKO
PCNT
γ–Tubulin
BF
M
GV
BD
MII
Exosc10-mVenus
EXO10-mV
BF/DAPI
1-Cell
2-Cell
Morula
Exosc10-mVenus
EXO10-mV
BF/DAPI
N
E1.5
E2.5
E3.5
Control
cKO
O
E1.5 embryos (%)
E2.5 embryos (%)
E3.5 embryos (%)
Control
cKO
N=48
N=30
1C
2C
1-2C
4C-Morula
1-4C
Morula-Blastocyst
Dead

Figure S2

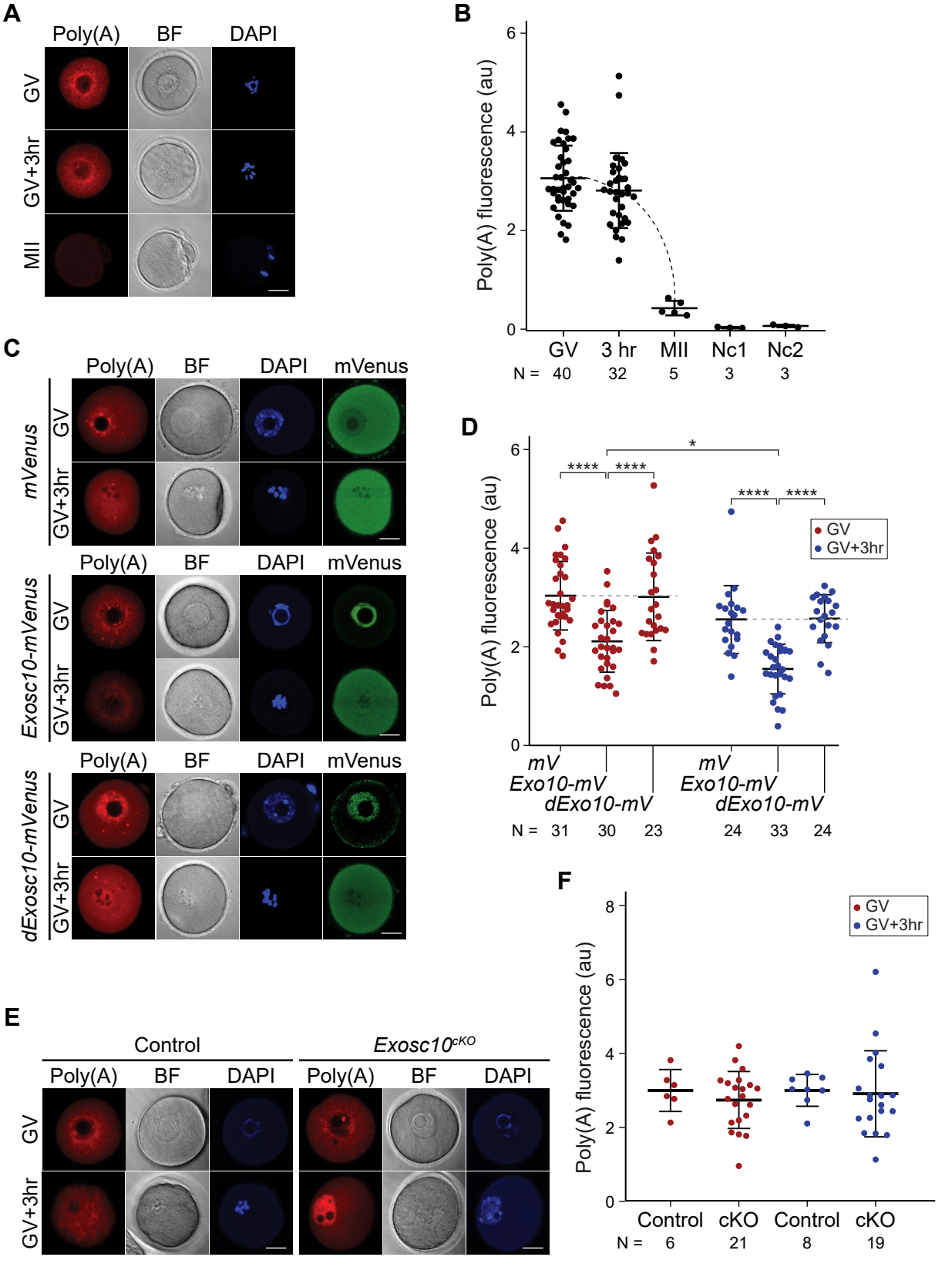
A
Poly(A)
BF
DAPI
GV
GV+3hr
MII
B
Poly(A) fluorescence (au)
GV
3 hr
MII
Nc1
Nc2
N = 40 32 5 3 3
C
Poly(A)
BF
DAPI
mVenus
mVenus
Exosc10-mVenus
dExosc10-mVenus
GV
GV+3hr
D
Poly(A) fluorescence (au)
****
*
GV
GV+3hr
mV
Exo10-mV
dExo10-mV
N = 31 30 23 24 33 24
E
Control
Exosc10cKO
Poly(A)
BF
DAPI
GV
GV+3hr
F
Poly(A) fluorescence (au)
GV
GV+3hr
Control
cKO
N = 6 21 8 19

Figure S3

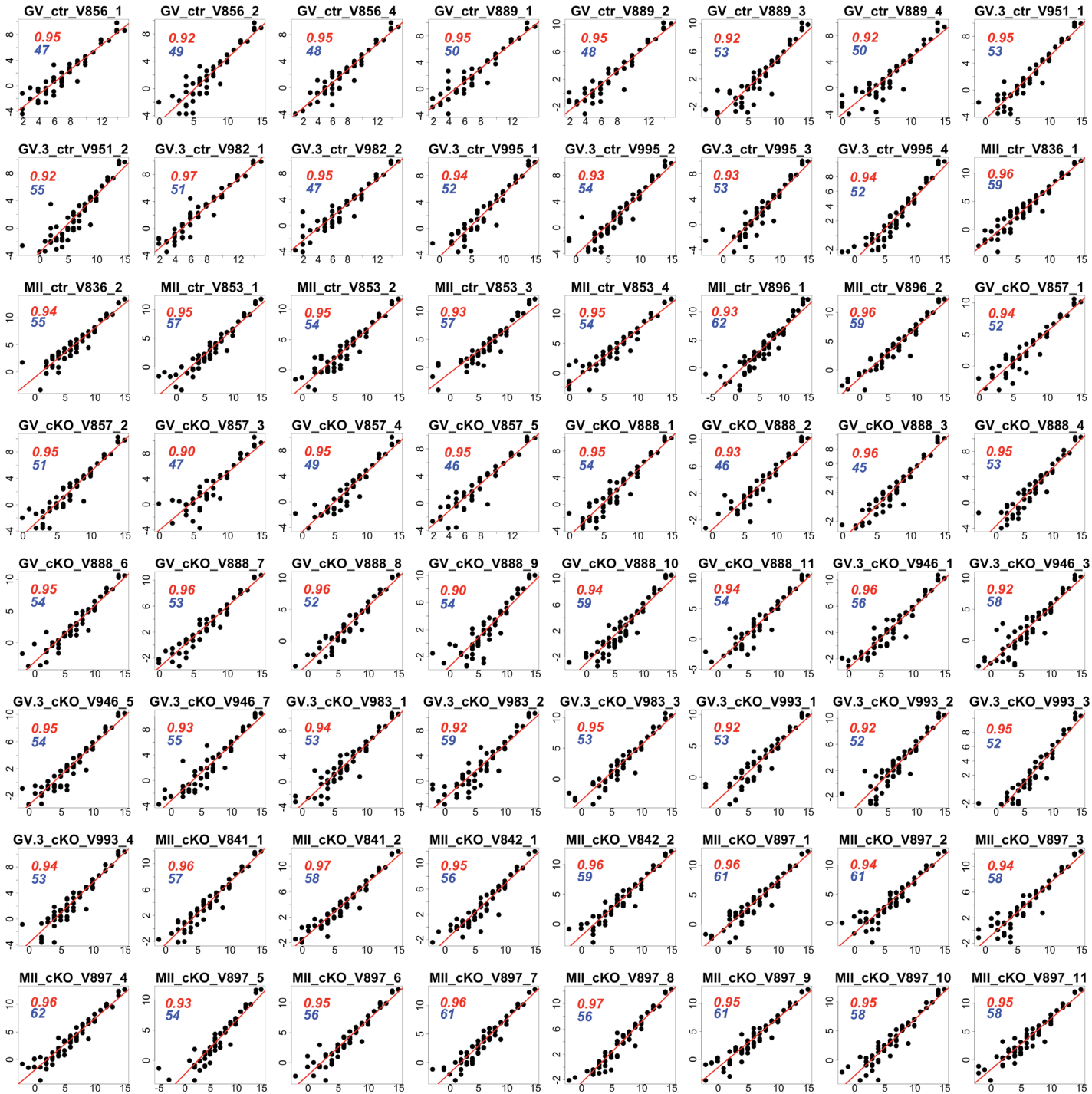
GV_ctr_V856_1
0.95
47
GV_ctr_V856_2
0.92
49
GV_ctr_V856_4
0.95
48
GV_ctr_V889_1
0.95
50
GV_ctr_V889_2
0.95
48
GV_ctr_V889_3
0.92
53
GV_ctr_V889_4
0.92
50
GV.3_ctr_V951_1
0.95
53
GV.3_ctr_V951_2
0.92
55
GV.3_ctr_V982_1
0.97
51
GV.3_ctr_V982_2
0.95
47
GV.3_ctr_V995_1
0.94
52
GV.3_ctr_V995_2
0.93
54
GV.3_ctr_V995_3
0.93
53
GV.3_ctr_V995_4
0.94
52
MII_ctr_V836_1
0.96
59
MII_ctr_V836_2
0.94
55
MII_ctr_V853_1
0.95
57
MII_ctr_V853_2
0.95
54
MII_ctr_V853_3
0.93
57
MII_ctr_V853_4
0.95
54
MII_ctr_V896_1
0.93
62
MII_ctr_V896_2
0.96
59
GV_cKO_V857_1
0.94
52
GV_cKO_V857_2
0.95
51
GV_cKO_V857_3
0.90
47
GV_cKO_V857_4
0.95
49
GV_cKO_V857_5
0.95
46
GV_cKO_V888_1
0.95
54
GV_cKO_V888_2
0.93
46
GV_cKO_V888_3
0.96
45
GV_cKO_V888_4
0.95
53
GV_cKO_V888_6
0.95
54
GV_cKO_V888_7
0.96
53
GV_cKO_V888_8
0.96
52
GV_cKO_V888_9
0.90
54
GV_cKO_V888_10
0.94
59
GV_cKO_V888_11
0.94
54
GV.3_cKO_V946_1
0.96
56
GV.3_cKO_V946_3
0.92
58
GV.3_cKO_V946_5
0.95
54
GV.3_cKO_V946_7
0.93
55
GV.3_cKO_V983_1
0.94
53
GV.3_cKO_V983_2
0.92
59
GV.3_cKO_V983_3
0.95
53
GV.3_cKO_V993_1
0.92
53
GV.3_cKO_V993_2
0.92
52
GV.3_cKO_V993_3
0.95
52
GV.3_cKO_V993_4
0.94
53
MII_cKO_V841_1
0.96
57
MII_cKO_V841_2
0.97
58
MII_cKO_V842_1
0.95
56
MII_cKO_V842_2
0.96
59
MII_cKO_V897_1
0.96
61
MII_cKO_V897_2
0.94
61
MII_cKO_V897_3
0.94
58
MII_cKO_V897_4
0.96
62
MII_cKO_V897_5
0.93
54
MII_cKO_V897_6
0.95
56
MII_cKO_V897_7
0.96
61
MII_cKO_V897_8
0.97
56
MII_cKO_V897_9
0.95
61
MII_cKO_V897_10
0.95
58
MII_cKO_V897_11
0.95
58

Figure S4

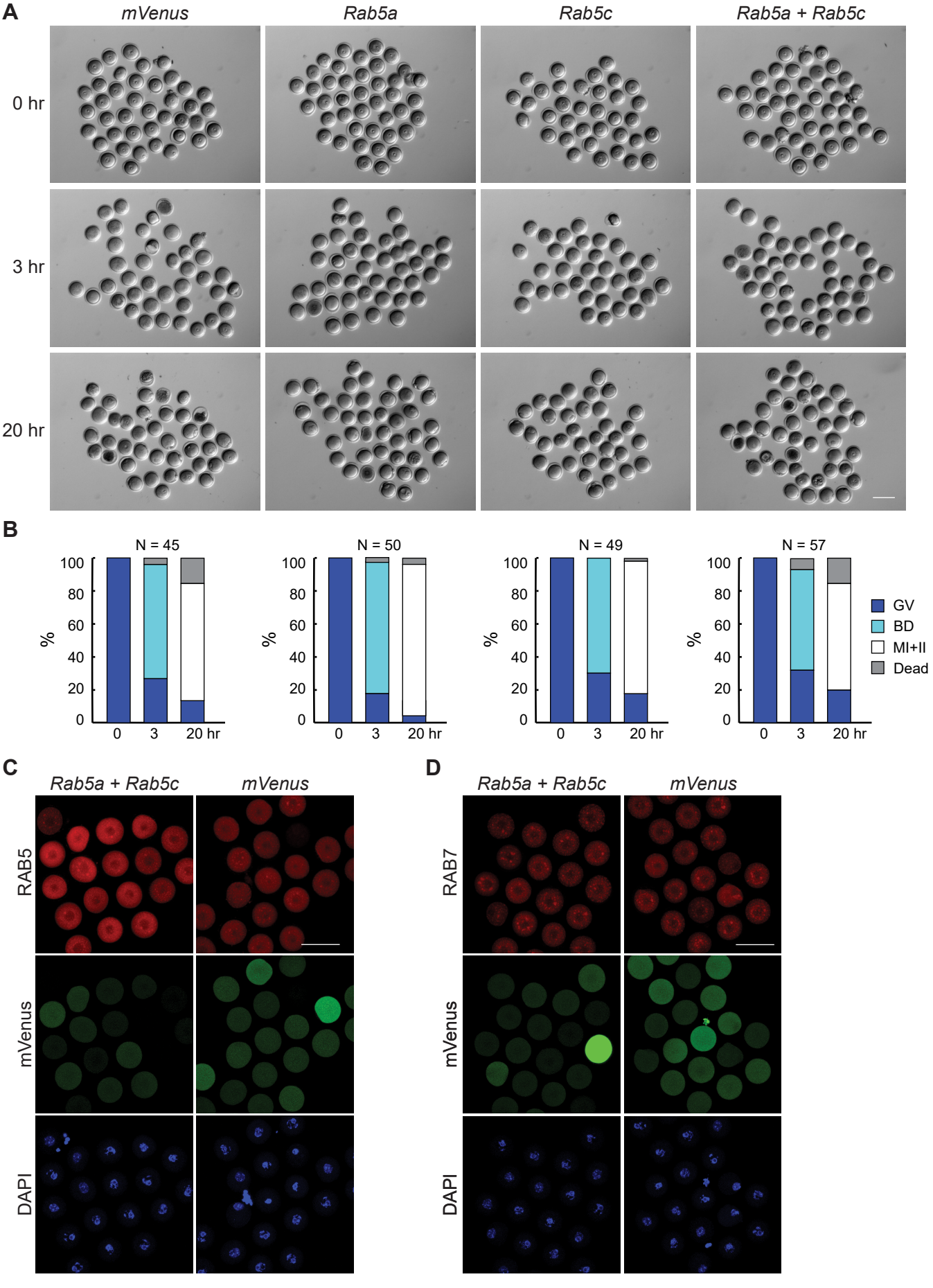
A
mVenus
Rab5a
Rab5c
Rab5a + Rab5c
0 hr
3 hr
20 hr
B
N = 45
N = 50
N = 49
N = 57
%
100
80
60
40
20
0
0
3
20 hr
GV
BD
MI+II
Dead
C
Rab5a + Rab5c
mVenus
RAB5
mVenus
DAPI
D
Rab5a + Rab5c
mVenus
RAB7
mVenus
DAPI

Figure S5

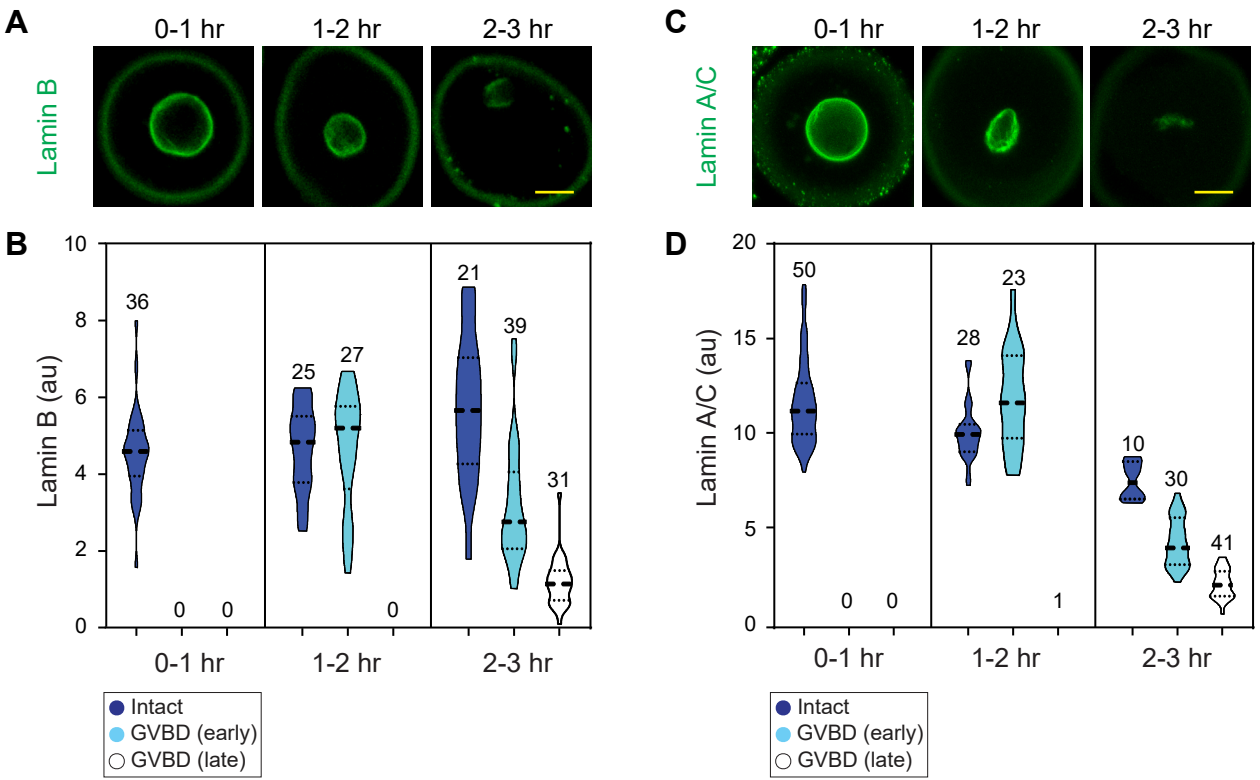
A
0-1 hr
1-2 hr
2-3 hr
Lamin B
C
0-1 hr
1-2 hr
2-3 hr
Lamin A/C
B
Lamin B (au)
10
8
6
4
2
0
36
0
0
25
27
0
21
39
31
0-1 hr
1-2 hr
2-3 hr
Intact
GVBD (early)
GVBD (late)
D
Lamin A/C (au)
20
15
10
5
0
50
0
0
28
23
1
10
30
41
0-1 hr
1-2 hr
2-3 hr
Intact
GVBD (early)
GVBD (late)

Figure S6

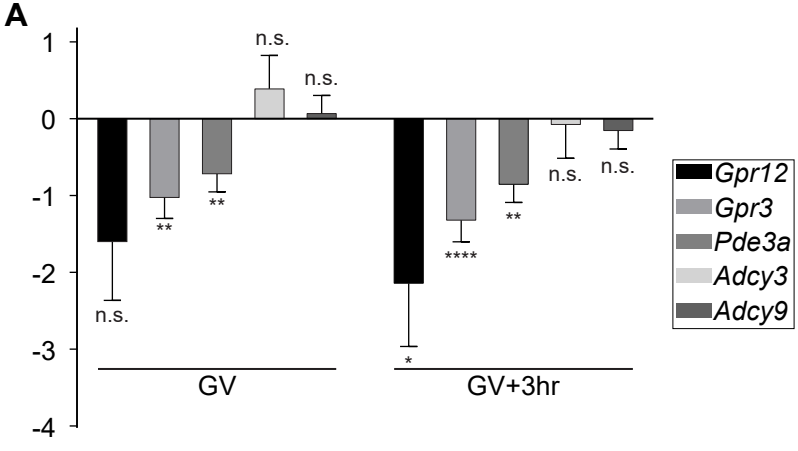
A
1
0
-1
-2
-3
-4
n.s.
n.s.
n.s.
**
**
****
**
n.s.
n.s.
*
GV
GV+3hr
Gpr12
Gpr3
Pde3a
Adcy3
Adcy9

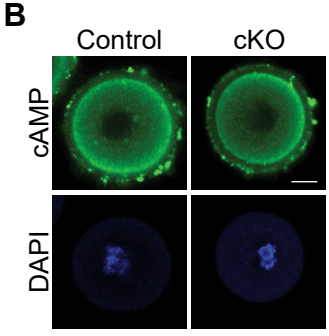
B
Control
cKO
cAMP
DAPI